Journal of Visualization, Vol. 10, No. 4 (2007)359-366

Regular Paper

Visualization of Turbulent Flow around a Sphere at Subcritical Reynolds Numbers

Jang, Y. I.* and Lee, S. J.*

* Department of Mechanical Engineering, Pohang University of Science and Technology, San 31, Hyoja-dong, Pohang, 790-784, Republic of Korea. E-mail: sjlee@postech.ac.kr

Received 5 April 2007
Revised 16 August 2007

Abstract : The shear layer evolution and turbulent structure of near-wake behind a sphere at Re =11,000 and 5,300 were investigated using a smoke-wire visualization method. A laminar flow separation was found to occur near the equator. The smooth laminar shear layers appeared to be axisymmetrically stable to the downstream location of about x/d = 1.0 at Re = 11,000 and x/d = 1.7~1.8 at Re = 5,300, respectively. At Re = 11,000, the vortex ring-shaped protrusions were observed with the onset of shear layer instability. Moreover, the transition from laminar to turbulence in the separated flow region occurred earlier at the hiher Reynolds number of Re = 11,000 than at Re = 5,300. The PIV measurements in the streamwise and cross-sectional planes at Re =11,000 clearly revealed the turbulent structures of the sphere wake such as recirculating flow, shear layer instability, vortex roll-up, and small-scale turbulent eddies.

Keywords : Sphere, Shear layer instability, Turbulent wake, Smoke-wire visualization.

1. Introduction

A sphere is considered as an idealized model of three-dimensional axisymmetric bluff bodies. Bluff bodies usually cause massive flow separation, unsteady flow, and complicated vortex shedding. Typical bluff bodies whose shape resembles a sphere include balloons, particles, towed sonars, bombs, oil-storage tanks, raindrops, and the like. It is well known that a sphere does not have a fixed flow separation point. Moreover, the separation point moves along the sphere surface depending on the outer flow condition and boundary layer developed on the sphere surface. Because a sphere is a basic body of which the flow structure is important for various practical applications, many visualization studies on the flow around a sphere have been conducted.

The flow around a sphere shows a steady axisymmetric flow in the range of Reynolds number 20 to 210. The axisymmetry is then broken, and planar-symmetric flow appears until Re = 280. From Re = 280, unsteadiness starts to occur in the planar-symmetric flow, and hairpin vortices are periodically shed. In the range of Reynolds number 420 to 800, asymmetric flow is observed, and unsteadiness continues (Taneda, 1956; Nakamura, 1976; Wu and Faeth, 1993; Leweke et al., 1999). Many researchers have visualized the sphere wake in this Reynolds number range in order to study laminar flow separation, symmetric flow pattern of near-wake, hairpin vortex shedding, and laminar wake. On the other hand, from Re = 800, the prominent flow phenomena are large-scale low-frequency vortex shedding and small-scale high-frequency shear layer instabilities (Kim and Durbin, 1988). A large-scale vortex is shed with a wavy shape, and turbulence occurs in the far field. At the critical Reynolds number of $Re = 3.7 \times 10^5$, the drag coefficient is rapidly reduced. This results from the sequential laminar separation, reattachment, and turbulence transition of the boundary layer on the sphere surface. The sphere wake becomes fully turbulent beyond this critical Reynolds number. In the subcritical Reynolds numbers from 800 to 3.7×10^5, the drag coefficient has almost a constant value, and the flow separates laminarily from the sphere. In addition, the Kelvin-Helmhortz instability occurs in the separating shear layer, and the wake becomes turbulent.

In the subcritical Reynolds number regime, only a few visualization studies on the turbulent flow around a sphere have been carried out. The turbulent flow around a sphere is not easy to visualize experimentally. This is attributed to several factors such as the supporting difficulty of a sphere in a wind tunnel test section, the large area of separated flow, the short time-scale of turbulence, and the three-dimensional complicated flow structure. In relation to this, Taneda (1978) visualized a sphere wake using smoke at $Re = 10^4 \sim 10^6$ and observed the large-scale helical structure of the sphere wake. Werlé (1980) employed the dye method to visualize the recirculating flow of wake and the shear layer instability of a ring-shaped vortex behind a sphere at $Re = 1.6 \times 10^4$. Kim and Durbin (1988) reported that a vortex roll-up could not be observed in their visualization study on sphere wake. Sakamoto and Haniu (1990) classified a flow pattern of sphere wake according to Strouhal number in $Re = 3 \times 10^2 \sim 4 \times 10^4$ and observed vortex tube pulsations in the vortex formation region. Recently, several numerical studies (Constantinescu and Squires, 2004; Yun et al., 2006) have been conducted on the turbulent flow around a sphere. However, these works have difficulties when it comes to the validation of their simulation results due to lack of experimental data. This implies that there are still strong demands for a more detailed experimental observation of sphere wake in the subcritical Reynolds number regime. In addition, as Meier (1999) pointed out, the unsteady 3D flow fields need an advanced visual display of experimental results. Especially, recent advancements in optical visualization techniques often lead to new insights in the analysis of complicated 3D flow phenomena (Hwang et al., 2005).

The main objective of the present study is to investigate some questioned issues by visualizing the instantaneous flow field of the sphere wake at Re = 11,000 and 5,300 using an improved smoke-wire method and 2D PIV velocity field measurement technique, in which flow separation, onset of shear layer instability, and small-scale turbulent eddies are visualized clearly. The experimental observation obtained in this work would enhance the understanding on the turbulent wake of a sphere and would be used for validating numerical predictions.

2. Experimental Methods

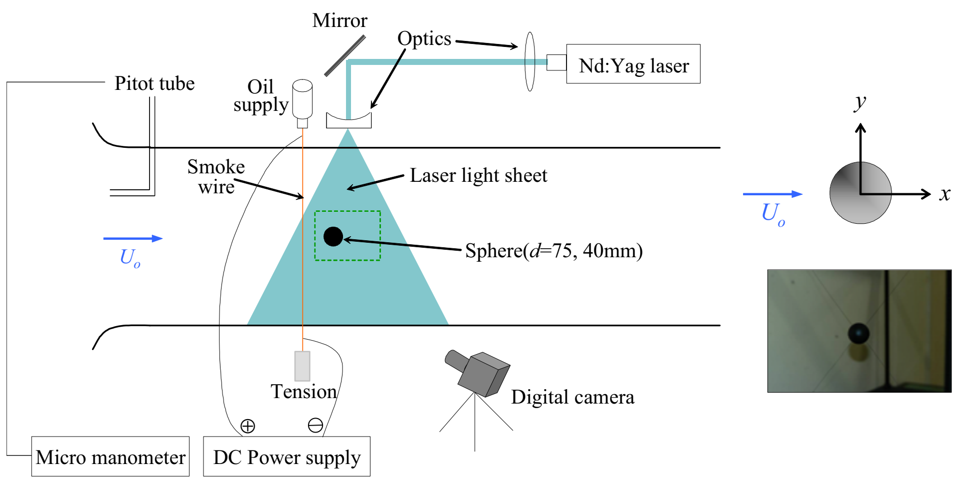

Fig. 1. Experimental setup for smoke-wire visualization and coordinate system.

Figure 1 shows the experimental setup for smoke-wire visualization in a closed-circuit wind tunnel, of which test section size is $6.75^{L} \times 0.72^{W} \times 0.6^{H}$ m^3. The freestream velocity was fixed at U_o = 2.2 m/s at which the turbulence intensity was below 0.08 %. The sphere models of 75 and 40 mm in diameter, made of acryl, were used as a test model. The sphericity of the spheres was 0.6 % and the surface uniformity was less than 0.1 %. The Reynolds numbers based on the freestream velocity and sphere diameters (d) were Re = 11,000 and 5,300.

To support the sphere model in the wind tunnel, the two piano wires of 0.17 mm in diameter were inserted through the sphere center in 'X' shape, facing upwards perpendicularly. The ends of the four wires were fastened firmly to the frame of the wind tunnel with precise turnbuckles. The blockage ratio of the sphere, including wires and frame, was below 2.5 %. The sphere supported at the center of the wind tunnel test section showed no visible vibration in the streamwise and cross-sectional planes at the freestream velocity tested in this study. The effect of flow disturbance by the supporting wires was negligible in the consideration of wire diameter and location of visualization planes. This method of supporting a sphere with fine piano wires was employed by Sakamoto and Haniu (1995) in their water channel tests. Cannon et al. (1993) also used this method to visualize flow around axisymmetric bodies in wind tunnel tests. If a sphere model was towed in a towing tank, the passage way should be long enough to ensure a steady target velocity. For the case of supporting with a rear rod, the sphere wake would be reattached to the supporting rod, distorting the downstream flow field.

A nichrome wire of 0.1 mm in diameter was used as a smoke-wire. White smoke filaments were generated by supplying electric voltage of 24 volt after coating Safex fog oil along the wire. Instantaneous snapshots on the flow field around a sphere were obtained after placing the smoke-wire at different locations before and behind the sphere model to closely examine the separated wake flow.

The key factor in obtaining clear images of turbulent 3D flow is to make the exposure time as short as possible, in addition to strong light intensity. The problem was resolved by using a pulse laser having very short pulse width (Lee and Lee, 1999). A laser pulse of 7 ns width was irradiated from a Nd:YAG laser(Beamtech, 50 mJ) and passed through optical lenses to generate a laser light sheet of 3 mm thickness. The illuminated flow images were captured consecutively with a digital camera(Nikon D100) with exposure at F3.5 and a shutter speed of 13. A 60 mm micro lens was attached in front of the camera. Using this experimental set-up, we could obtain clear streaklines of flow around the sphere model.

In addition, to examine in depth the time-averaged turbulent structure of the sphere wake at the same Reynolds number of Re = 11,000, PIV measurements were carried out in a circulating water channel of $4.5^{L} \times 1.0^{W} \times 1.0^{H}$ m^3 in physical size. The PIV system consists of a two-head Nd:YAG laser of 125 mJ and a CCD camera of 2K × 2K pixels spatial resolution. For the streamwise plane measurement, the streamwise center plane was illuminated simultaneously from both the upper and lower sides of the test section to remove any shaded region. For the PIV measurements in cross-sectional planes, the CCD camera was inserted into a water-resistant case and installed at a far downstream inside the test section. The orthogonal in-plane velocity components (V_y, V_z) in the cross-sectional plane were decomposed into the radial and circumferential velocity components (V_r, V_θ) in the polar coordinate. Five hundred pairs of PIV particle images were captured at a sampling rate of 4Hz for each experimental condition. The two-frame cross-correlation algorithm was employed to extract instantaneous velocity vector fields from the particle images.

3. Results and Discussion

Figure 2 shows the instantaneous flow visualizations around a sphere model at Re = 11,000, which were obtained with smoke-wire positioned (a) ahead of and (b) behind the sphere model. In order to capture the separated flow region more clearly, the smoke-wire was positioned behind the sphere, especially to visualize the recirculating flow in near-wake. In all figs, the flow direction is from left to right. As shown in Fig. 2(b), the recirculating region formed behind the sphere is clearly visualized by smoke filaments convected upstream by reverse flow. Similar flow phenomena of this recirculating flow behind axisymmetic bodies were visualized by Cannon et al. (1993) on the wake behind a disk at $Re = 1.32 \times 10^4$ and by Kim and Durbin (1988) on the sphere wake at $Re = 3.2 \times 10^4$. The abscissa x/d in photographs represents the downstream distance from the center of the sphere model normalized by the sphere diameter.

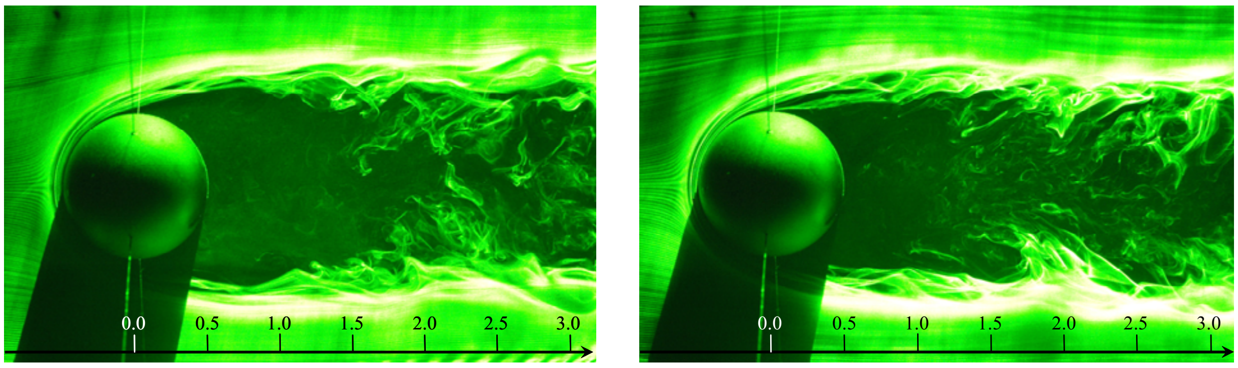

(a) Smoke-wire positioned ahead of a sphere

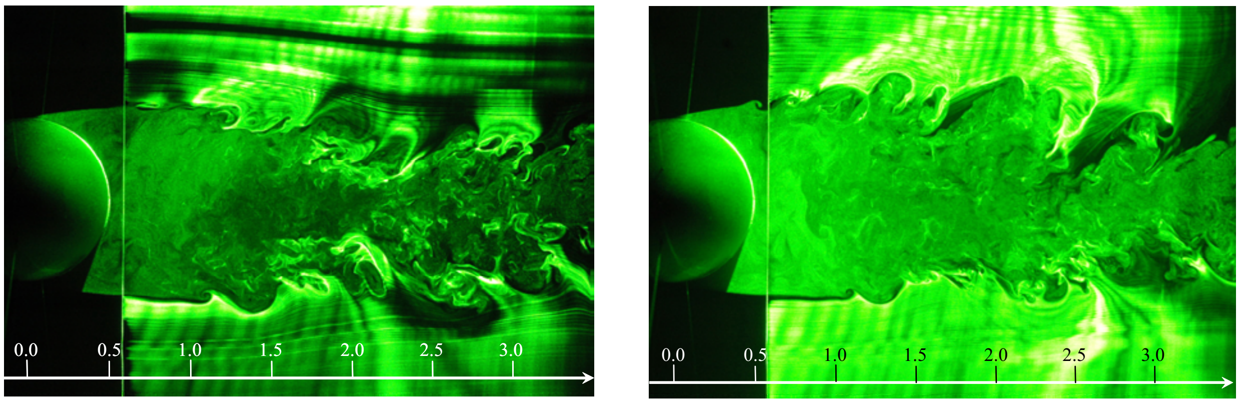

(b) Smoke-wire positioned behind a sphere

Fig. 2. Instantaneous flow fields visualized around a sphere at Re = 11,000.

In Fig. 2, the laminar flow separation occurs near the equator of the sphere model. On this location of laminar flow separation, Achebach (1972) reported the separation angle as 82.5° by measuring the shear stress in the subcritical Reynolds number regime. Constantinescu and Squires (2004) and Yun et al. (2006) found that the separation angle is 84° and 90°, respectively, by numerical simulations. In Fig. 2(b), the laminar shear layer continues until $x/d = 1.0 \sim 1.2$. At this point, the shear layer becomes unstable due to the Kelvin-Helmholtz (K-H) instability caused by a large velocity difference at the interface between the freestream and sphere wake. Thereafter, the laminar shear layer turns into turbulent flow. The vortex-ring shaped protrusions are observed at $Re = 11{,}000$, which are very similar to those shown in the works of Werlé (1980) at Re = 16,000 and Yun et al. (2006) at Re = 10,000. Meanwhile, Leder and Geropp (1993) observed the axisymmetric K-H instability at $x/d \approx 1.0$, but the ring-type protrusions were not observed at Re = 10,000. In the visualization study of Hadzic et al. (2002) at $Re = 5 \times 10^4$, the K-H instability occurred near $x/d \approx 0.6$, and the laminar wake quickly changed into turbulent flow. This kind of wide scattering of flow separation angle and onset location of shear layer instability seems to result from the difference in freestream turbulence intensity, sphere supporting methodology, and different turbulence models employed in the numerical simulations.

Figure 3 represents the visualized images of instantaneous flow around a sphere at $Re = 5{,}300$, with installation of smoke-wire at three downstream locations. As shown in Figs. 3(a) and (b), the flow also separates laminarily near the equator of the sphere model. The separated shear layers progress axisymmetrically and appear to be stable in the downstream flow field. The K-H instability occurs near x/d = 1.7 ~ 1.8. The present results of the separation angle and onset location of shear layer instability agree well with those of Sakamoto et al. (1990) at Re = 4,460. Moreover, the flow separation angle is in good agreement also with that in the work of Seidl et al. (1998) at Re = 5,000. However, the transition occurs a little earlier in their work.

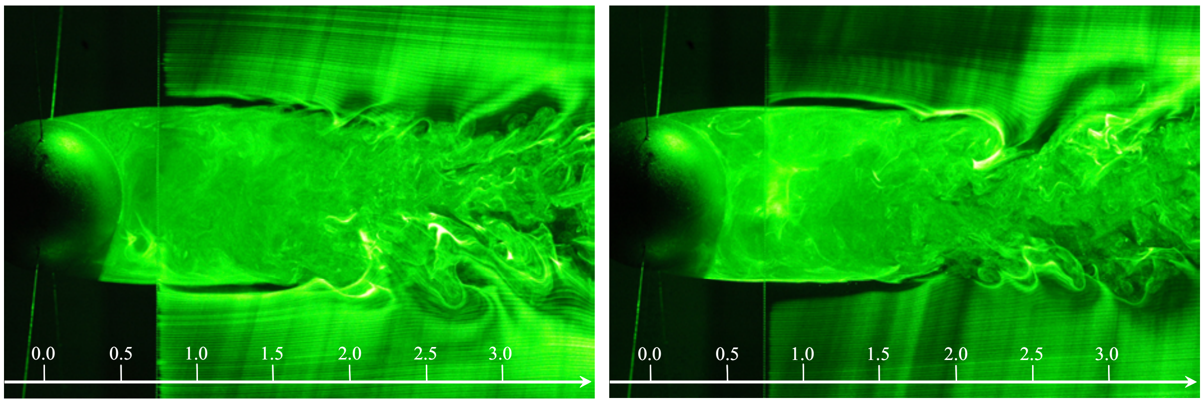

(a) Smoke-wire positioned at x/d = 0.75

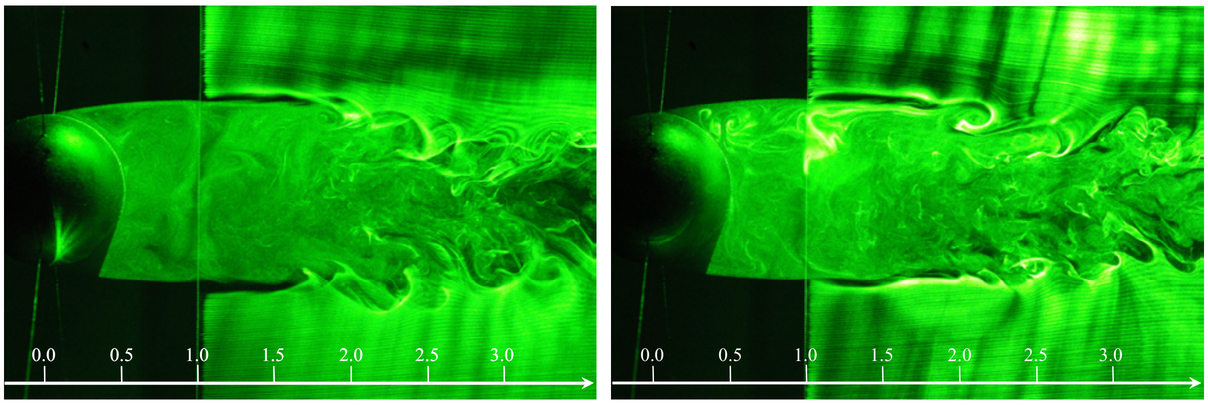

(b) Smoke-wire positioned at x/d = 1.0

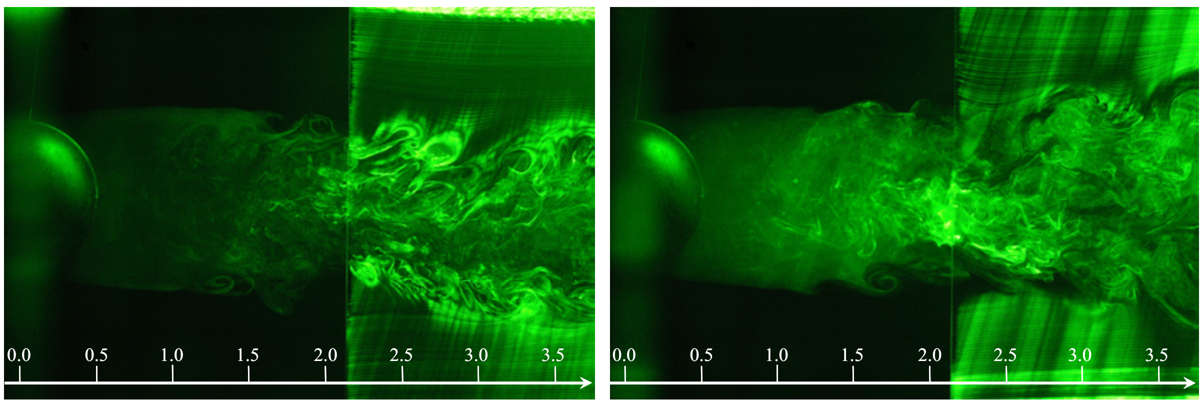

(c) Smoke-wire positioned at x/d = 2.2

Fig. 3. Instantaneous flow fields visualized around a sphere at Re = 5,300.

Comparing Fig. 2(b) and Figs. 3(a)-(b), the transition to turbulent in the separating shear layers and the onset of wavy wake occur earlier at Re = 11,000 than at Re = 5,300. The vortex roll-up breaks into small-scale vortices to feed the turbulent wake. Furthermore, the number of small-scale vortices at Re = 11,000 is more than at Re = 5,300. This implies fast energy transport into the vortex formation region at a higher Reynolds number. It is also worthy to note that the turbulent wake past the transition region exhibits strong fluctuations and a chaotic flow structure at Re = 11,000.

Figure 3(c) shows that the recirculating region filled with smoke filaments convected upstream behind the sphere is observed until the location of smoke-wire at x/d = 2.2. This indicates clearly the existence of reverse flow and the length of the vortex formation region. In the numerical results of the work of Seidl et al. (1998) simulated at Re = 5,000, the reverse flow was observed up to the location of x/d = 2.0 and disappeared just before the flow passes the location of x/d = 2.5. Therefore, it seems that Fig. 3(c) reasonably agrees with the DNS prediction.

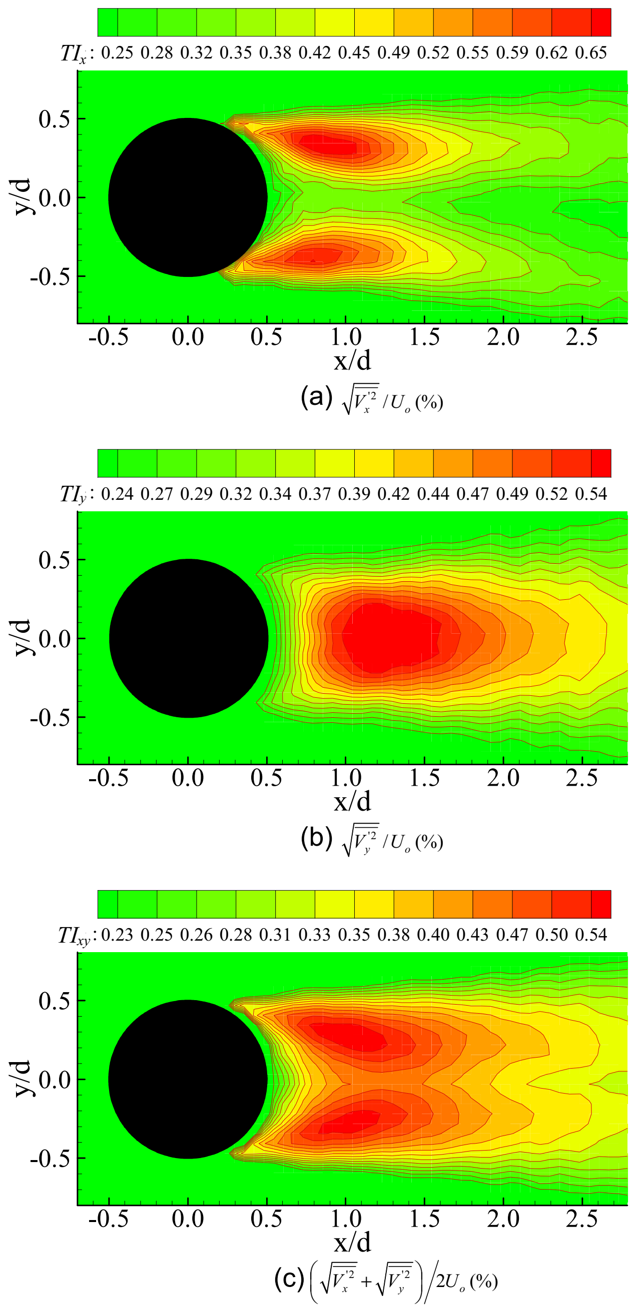

Fig. 4. Spatial distributions of turbulence intensities of sphere wake in the streamwise plane at Re = 11,000.

Figure 4 shows the spatial distributions of the turbulence intensities measured using a 2D PIV system. The streamwise turbulence intensity has the local maximum value at *x/d* = 0.85 and *y/d* = ±0.35, around which elliptic-shaped contours are formed inside the recirculating flow region. Their magnitude is gradually dissipated as the flow goes downstream. In Fig. 4(b), the vertical turbulence intensity has the local maximum value at *x/d* =1.2 along the wake centerline (y = 0). Leder and Geropp (1993) measured the mean squares of fluctuating velocities $\left(\sqrt{\overline{V_x'^2}}\text{ and }\sqrt{\overline{V_y'^2}}\right)$ at $Re = 5 \times 10^4$ using an LDA system. Their results are similar with the present results except for the fact that the maximum turbulence intensities of $\sqrt{\overline{V_x'^2}}$ and $\sqrt{\overline{V_y'^2}}$ occur at *x/d* = 1.0 and 1.4, respectively. The spatial distribution of $\left(\sqrt{\overline{V_x'^2}}+\sqrt{\overline{V_y'^2}}\right)$ has large values in tilted elliptic-shaped contours as shown in Fig. 4(c), and the local maximum value occurs at *x/d* = 1.05. The regions of large turbulent statistical values seem to be closely related to the onset of shear layer instability in the near-wake behind the sphere model. Especially, the location of the local maximum value $\left(\sqrt{\overline{V_x'^2}}+\sqrt{\overline{V_y'^2}}\right)$ in Fig 4(c) corresponds to the onset location of shear layer instability in Fig. 2(b).

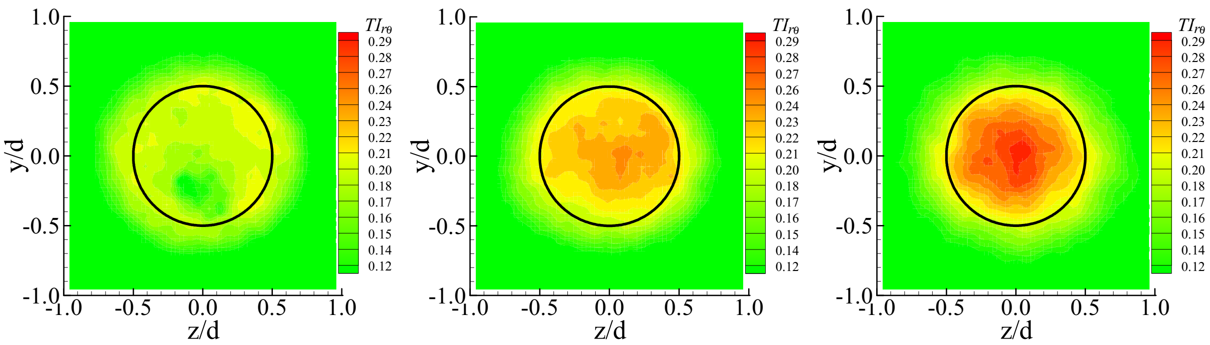

(a) *x/d* = 0.8 (b) *x/d* = 1.0 (c) *x/d* = 1.2

Fig. 5. Contour plots of the total in-plane turbulence intensity $\left(\sqrt{\overline{V_r'^2}}+\sqrt{\overline{V_\theta'^2}}\right)/2U_o\,(\%)$ of sphere wake in cross- sectional planes at *Re* = 11,000.

The spatial distributions of the total in-plane turbulence intensity $\left(\sqrt{\overline{V_r'^2}}+\sqrt{\overline{V_\theta'^2}}\right)$ measured using the 2D PIV system of three cross-sectional planes of *x/d* = 0.8, 1.0 and 1.2 are shown in Fig. 5. It has large values around the sphere periphery at *x/d* = 0.8. With going downstream, the regions of large turbulence intensity move toward the wake center, and it has the maximum value at *x/d* = 1.2. These PIV results confirm that the sphere wake is a three-dimensional flow and there exists shear-layer instability in the cylinder-shaped region of sphere periphery behind the sphere model.

4. Conclusion

Turbulent flow around a sphere at *Re* = 11,000 and 5,300 in the subcritical Reynolds number regime was visualized using the smoke-wire technique. Clear flow images were obtained by employing a strong laser light sheet with a very short duration to irradiate the measurement planes. Laminar flow separation occurred near the sphere equator at both *Re* = 11,000 and 5,300. The laminar shear layer was axisymmetically stable to the downstream location of *x/d* = 1.0 ~ 1.2 at *Re* = 11,000 and *x/d* = 1.7 ~ 1.8 at *Re* = 5,300, respectively.

In addition, the PIV measurements in the streamwise and cross-sectional planes at *Re* = 11,000 revealed the turbulent structure of the sphere wake. The PIV results of time-averaged turbulent structures were consistent with the visualized flow showing the onset of shear layer instability. At *Re* = 11,000, vortex ring-shaped protrusions began to appear with the onset of the shear layer instability. The transition from laminar to turbulent and the onset of wavy wake structure occurred earlier at *Re* = 11,000 than at *Re* = 5,300. Moreover, a greater number of small-scale vortices as well as strong velocity fluctuations and more chaotic flow structure were identified at *Re* = 11,000. The detailed turbulent structure of sphere wake such as recirculating flow, shear layer instability, vortex roll-up, and small-scale turbulent eddies were clearly visualized in this study.

Acknowledgments

This work was supported by the Korea Science and Engineering Foundation (KOSEF) through the National Research Lab. Program funded by the Ministry of Science and Technology (No. M10600000 276-06J0000 -27610).

References

Achebach, E., Experiments on the Flow past Spheres at Very High Reynolds Numbers, Journal of Fluid Mechanics, 54-3 (1972), 565-575.

Cannon, S., Champagne, F. and Glezer A., Observations of Large-scale Structures in Wakes behind Axisymmetric Bodies, Experiments in Fluids, 14-6 (1993), 447-450.

Constantinescu, G. S. and Squires, K. D., Numerical Investigations of Flow over a Sphere in the Subcritical and Supercritical Regimes, Physics of Fluids, 16-5 (2004), 1449-1466.

Hadzic, I., Bakić, V., Perić, M., Sajn, V. and Kosel F., Experimental and Numerical Studies of Flow around Sphere at Sub-critical Reynold Number, Engineering Turbulence Modeling and Experiments-5 (2002), 667-676.

Hwang, T. G., Doh, D. H. and Okamoto K., 4D-PTV: Measurements of an Impinged Jet with a Dynamic 3D-PTV, Journal of Visualization, 8-3 (2005), 245-252.

Kim, H. J. and Durbin, P. A., Observations of the Frequencies in a Sphere Wake and of Drag Increase by Acoustic Excitation, Physics of Fluids, 31-11 (1988), 3260-3265.

Leder, A. and Geropp, D., The Unsteady Flow Structure in the Wake of the Sphere, SPIE, 2052 (1993), 119-126.

Lee, S. J. and Lee, S. H., Synchronized Smoke-wire Technique for Flow Visualization of Turbulent Flows, Journal of Flow Visualization and Image Processing, 6 (1999), 65-78.

Leweke T., Provansal M., Ormières D. and Lebescond R., Vortex Dynamics in the Wake of a sShere, Physics of Fluid, 11-9 (1999), S12.

Meier, G. E. A., Optical Tools for Aerodynamics, Journal of Visualization, 2-1 (1999), 51-58.

Nakamura, I., Steady Wake behind a Sphere. Physics of Fluids, 19-1 (1976), 5-8.

Sakamoto, H. and Haniu, H., A Study on Vortex Shedding from Spheres in a Uniform Flow. Journal of Fluids Engineering, 112 (1990), 386-392.

Sakamoto, H. and Haniu, H., The Formation Mechanism and Shedding Frequency of Vortices from a Sphere in Uniform Shear Flow. Journal of Fluid Mechanics, 287 (1995), 151-171.

Seidl, V., Muzaferija, S. and Perić, M., Parallel DNS with Local Grid Refinement, Applied Scientific Research, 59 (1998), 379-394.

Taneda, S., Experimental Investigation of the Wake behind a Sphere at Low Reynolds Number, Journal of the Physical Society of Japan 11-10 (1956), 1104-1108.

Taneda, S., Visual Observations of the Flow past a Sphere at Reynolds Numbers between 10^4 and 10^6, Journal of Fluid Mechanics, 85-1 (1978), 187-192.

Werlé, H., ONERA Photograph In: An Album of Fluid Motion (edited by Dyke, V.), (1980), 32-35, Parabolic Press.

Wu, J. S. and Faeth, G. M., Sphere Wakes in Still Surroundings at Intermediate Reynolds Numbers, AIAA J., 31-8 (1993), 1448-1455.

Yun G., Kim D. and Choi H., Vortical Structures behind a Sphere at Subcritical Reynolds Numbers, Physics of Fluids, 18-1 (2006), 015102.

Author Profile

Sang Joon Lee: He received his Master's and Ph.D. degrees in Mechanical Engineering from KAIST in 1982 and 1986, respectively. In 1986, he worked as a senior researcher at KIMM. He is currently a professor in the Department of Mechanical Engineering at POSTECH, which he has been with since 1987. His research interests are quantitative flow visualization (PIV, PTV, LIF, Holography, X-ray imaging), experimental fluid mechanics, bluff body aerodynamics, microfluidics, and bio-fluid flows.

Young Il Jang: He graduated from ROK Air Force Academy in 1995 and received his M.Sc. degree in Aerospace Engineering in 1998 from the Georgia Institute of Technology. After obtaining his M.Sc. Degree, he worked as an instructor at ROK Air Force Academy and is now working on his Ph.D degree at POSTECH, majoring in experimental fluid mechanics. His current research interest is the investigation of turbulent flow around a sphere.